The Ctf18 RFC-like complex positions yeast telomeres but does not specify their replication time

Shin-ichiro Hiraga, E Douglas Robertson and Anne D Donaldson*

Institute of Medical Sciences, University of Aberdeen,

Foresterhill, Aberdeen AB25 2ZD, Scotland, UK.

Running Title: The Ctf18-RLC positions yeast telomeres

*Corresponding author; E-mail: a.d.donaldson@abdn.ac.uk

[Keywords: Ctf8/Dcc1/Ku/SIR proteins]

Suggested Subject Categories:

1. Genome Stability & Dynamics
2. Chromatin & Transcription

Total Number of Characters (excluding title page): 48080

Chromosome ends in *Saccharomyces cerevisiae* are positioned in clusters at the nuclear rim. We report that Ctf18, Ctf8, and Dcc1, the subunits of a Replication Factor C-like complex, are essential for the perinuclear positioning of telomeres. In both yeast and mammalian cells peripheral nuclear positioning of chromatin during G1 phase correlates with late DNA replication. We find that the mislocalized telomeres of *ctf18* cells still replicate late, showing that late DNA replication does not require peripheral positioning during G1. The Ku and Sir complexes have been shown to act through separate pathways to position telomeres, but in the absence of Ctf18 neither pathway can act fully to maintain telomere position. Surprisingly *CTF18* is not required for Ku or Sir4-mediated peripheral tethering of a non-telomeric chromosome locus. Our results suggest that the Ctf18 Replication Factor C-like complex modifies telomeric chromatin to make it competent for normal localization to the nuclear periphery.

Introduction

The physical organization of DNA within the nucleus is related to chromatin function. Chromosomes of higher eukaryotes occupy specific nuclear 'territories', and the spatial territory of a chromosome frequently reflects its gene-density, with chromosomes containing a high proportion of non-transcribed sequence located close to the edge of the nucleus (Tanabe et al, 2002). Although it is clear that chromatin is organized and actively positioned within the nuclear space, the mechanisms determining physical organization of chromosomes within nuclei are not understood.

All eukaryotic cells replicate their DNA according to a reproducible temporal program and spatial organization of the DNA is correlated with replication timing (reviewed in Taddei et al, 2004b). Replication foci are typically spread throughout the nuclear interior during early S phase, while peripheral and perinucleolar DNA replicates in mid to late S

phase. Non-expressed heterochromatic DNA usually replicates late in S phase (Gilbert et al, 2004; Woodfine et al, 2004). In general, the spatial organization, transcriptional activity and replication timing of chromatin are correlated, but causative relationships between these three properties are unclear.

The organization of the telomeres of *S. cerevisiae* offers a useful model system for studying chromosome positioning, transcriptional activity, and replication timing. The 32 telomeres of haploid yeast cells associate in 3 to 6 clusters at the nuclear periphery (Gotta et al, 1996). *S. cerevisiae* subtelomeric sequences are subject to silencing of polymerase II-mediated transcription (Gottschling et al, 1990) and telomeres are replicated late during S phase (Ferguson and Fangman, 1992; Raghuraman et al, 2001).

Two partially redundant pathways have been identified that mediate tethering of telomeres to the nuclear rim. The first depends on the yeast Ku (yKu) protein complex (which consists of Yku70 and Yku80 proteins), and the second on the Sir4 and Esc1 proteins (Hediger et al, 2002; Taddei et al, 2004a). Different telomeres may differ somewhat in their dependence on these two pathways—for example during G1, telomere VI-right (VIR) positioning depends primarily on the Ku pathway and telomere VI-left (VIL) primarily on the Sir4/Esc1 pathway (Bystricky et al, 2005). Some evidence suggests that the Ku-dependent pathway tends to dominate during G1, while the Sir4/Esc1-dependent tethering pathway is dominant in S phase (Hediger et al, 2002). The telomeres lose their peripheral localization during G2 as cells prepare to enter mitosis, and perinuclear positioning is re-established in early G1 phase. However, the telomere positioning mechanism is not fully understood, and in particular the molecular components that act with Ku to mediate telomere positioning are not known. Identification of additional positioning components is complicated by the fact that Ku also plays a key role in other telomere-specific functions including subtelomeric transcriptional silencing (Gravel et al, 1998; Laroche et al, 1998), telomerase recruitment

(Stellwagen et al, 2003) and specification of late replication timing (Cosgrove et al, 2002).

Peripheral localization of DNA within the yeast nucleus has been shown to reinforce transcriptional silencing in a number of cases. For example, artificial localization to the periphery enhances transcriptional repression at a compromised silencer (Andrulis et al, 1998). Consistently, both Ku and *SIR4* are required for maximum silencing of subtelomeric genes (Gravel et al, 1998; Laroche et al, 1998; Palladino et al, 1993). However, under some circumstances positioning and silencing can be separated. Repression can be maintained at an intact silencer that is released from the nuclear peripheral zone (Gartenberg et al, 2004), and at a modified version of telomere VIIL there was no correlation between proportion of peripherally positioned telomeres and the efficiency of silencing (Tham et al, 2001).

The relationship between peripheral localization and replication timing has been less investigated. The telomeres and ribosomal DNA are localized close to the nuclear envelope and replicate in the second half of S phase (Raghuraman et al, 2001; A. Cosgrove & A. Donaldson, unpublished), suggesting that peripheral localization may favor late replication. Moreover, removal of Ku function leads simultaneously to delocalization and abnormally early replication of telomeres (Cosgrove et al, 2002). Localization of the DNA during G1 phase has been proposed to be particularly crucial for correct timing control (Gilbert, 2002), since the *S. cerevisiae* telomere late replication program is pre-established during G1 (Raghuraman et al, 1997). The replication program in mammalian cells is also established during G1 coincident with re-positioning of DNA within the nucleus (Dimitrova and Gilbert, 1999).

Replication factor C (RFC) is a five subunit 'clamp-loading' complex consisting of the essential gene products Rfc1-5, all of which belong to the AAA+ ATPase superfamily (Bowman et al, 2004). RFC loads the ring-shaped PCNA polymerase clamp component of replication forks. Three RFC-like complexes have been identified in which the largest subunit

(Rfc1) is replaced by either Rad24, Ctf18, or Elg1; *RAD24*, *CTF18*, and *ELG1* are non-essential genes with sequence similarity to *RFC1* (reviewed in Kim and MacNeill, 2003). The Elg1 and Rad24 Replication Factor C-like complexes (Elg1-RLC and Rad24-RLC) are important for genome stability and checkpoint responses, and Rad24-RLC has been shown to load the ring-shaped 9-1-1 complex onto damaged DNA. The Ctf18-RLC is a heptameric complex containing two extra subunits, Ctf8 and Dcc1, in addition to Rfc2-5 and Ctf18 itself. The function of Ctf18-RLC remains mysterious. Disruption of either *CTF18*, *CTF8*, or *DCC1* causes a sister chromatid cohesion defect, but no cohesin loading defect was detected in a *ctf8* mutant (Hanna et al, 2001; Kenna and Skibbens, 2003; Mayer et al, 2001). By analogy to RFC and the Rad24-RLC, the Ctf18-RLC is believed to act on a ring-shaped complex. Human Ctf18-RLC can load PCNA *in vitro*, although with reduced efficiency when compared to RFC itself (Bermudez et al, 2003; Merkle et al, 2003; Ohta et al, 2002). It has recently been demonstrated that yeast Ctf18-RLC efficiently unloads PCNA from DNA *in vitro* (Bylund and Burgers, 2005).

Here we show that Ctf18-RLC mediates correct positioning of yeast telomeres at the nuclear periphery. Despite the disruption of telomere peripheral positioning, the telomeres of *ctf18* cells replicate late in S phase, showing that peripheral positioning during G1 is not required for late replication of DNA. We propose that the Ctf18-RLC may act, through unloading of PCNA and/or exchange of PCNA-like ring-shaped complexes, to establish a chromatin structure that is required for telomere positioning.

Results

The Ctf18-RLC complex is required for perinuclear positioning of Rap1

To elucidate molecular mechanisms responsible for positioning chromatin within the nucleus,

we screened for new gene products involved in localizing *S. cerevisiae* telomeres. The screen will be described in detail elsewhere; briefly, it is based on examining the subnuclear localization of the telomeric heterochromatin component Rap1. We transformed a series of disruption mutants in non-essential genes with a plasmid encoding GFP-Rap1, and screened for those mutants in which GFP-Rap1 localization appeared abnormal. Expression of GFP-Rap1 in wild-type cells (Hayashi et al, 1998) reveals several discrete dots corresponding to the telomere clusters (Figure 1). In unbudded and small-budded cells these dots are predominantly localized at the nuclear rim, as expected since telomeres are localized to the nuclear periphery during the early part of the cell cycle. The Ku complex is required for correct localization of telomeres. As a control for the effect of telomere localization on Rap1 positioning, we confirmed that the Rap1 foci were largely dispersed in a *yku70* strain (Figure 1). On examination of a *ctf18* strain we found that GFP-Rap1 foci were almost completely disrupted, with the Rap1-GFP signal dispersed throughout the nuclear interior (Figure 1). As described above, the Ctf18-RLC is a seven subunit RFC-like complex that includes the gene products Ctf8 and Dcc1. We found that Rap1 foci were also dispersed in *ctf8* and *dcc1* mutants (Figure 1). The fact that the *ctf18*, *ctf8*, and *dcc1* mutants all share the same Rap1 localization defect suggests that the Ctf18-RLC is essential for proper Rap1 localization to the nuclear periphery, rather than the effect being due to one of the gene products alone.

Rad24 and Elg1 are the largest subunits of the two other RLC complexes. Neither *rad24* nor *elg1* mutant showed a GFP-Rap1 localization defect (Figure 1), suggesting that the role in Rap1 localization within the nucleus is specific to Ctf18-RLC.

The Ctf18-RLC is required for telomere positioning

One possible interpretation of the results in Fig. 1 is that the Ctf18-RLC is required for telomere positioning. To address this possibility, we tested the effects of deleting *CTF18*,

CTF8, or *DCC1* on telomeres that were fluorescently tagged (Straight et al, 1996). We used a strain in which a single telomere is marked by GFP fused to the *lac* repressor and the nuclear envelope is simultaneously visualized by GFP tagging of a nuclear pore component, so that the telomere is visible as a bright dot within a circle corresponding to the nuclear envelope (Figure 2A). In the majority of interphase wild-type cells, the telomere dot appears to touch the nuclear envelope (corresponding to a distance of less than 230 nm). Telomeres VIR, VIIIL, and XIVL were localized at the nuclear rim in a reduced proportion of *ctf18*, *ctf8*, and *dcc1* cells, with levels of localization similar to those of a *yku70* mutant (Figure 2B). The *CTF18*, *CTF8*, and *DCC1* gene products are therefore required for correct positioning of *S. cerevisiae* telomeres at the nuclear periphery.

To test whether another peripherally localized sequence is disrupted in *ctf18* cells, we examined the distribution of the ribosomal DNA which is normally packaged at the edge of the nucleus. Observation of the rDNA using a GFP-tagged Net1 protein (which binds the ribosomal DNA repeats) revealed no apparent mislocalization of the rDNA (data not shown). Nuclear structure therefore does not appear to be grossly disrupted in the *ctf18* mutant.

CTF18 is required for telomere localization in G1 and S phase

To assess the cell cycle stages at which Ctf18 is important for telomere localization, we examined telomere position in cells scored for cell cycle position according to bud size. We quantified the position of telomere XIVL by dividing the nucleus into three concentric zones of equal area (Figure 3A) as described (Taddei et al, 2004a). In this assay random telomere positioning would be represented by 33% of telomeres scored in each zone. In wild-type nuclei, telomere XIVL preferentially localizes to the outermost zone in both G1 and S phase (Figure 3B and Table I). In *ctf18* G1 phase nuclei, the same telomere was almost randomly positioned (39% of telomeres in Zone 1: Figure 3B and Table I). Once *ctf18* cells entered S

phase, the telomere remained slightly delocalized from the periphery when compared to wild-type, although the effect was not as severe as in G1. χ^2 analysis confirmed that telomere position during S phase in *ctf18* is significantly different from that of WT and from random distribution. Very similar cell cycle effects were observed for telomere VIIIL (localization to Zone 1 in 67% of wt G1 cells, 32% of *ctf18* G1 cells, 61% of wt S cells, and 49% of *ctf18* S cells). P values assessing the statistical significance of these results are given in Table I. We conclude that telomere positioning is affected by *CTF18* deletion primarily in G1 phase cells, with absence of Ctf18 being slightly deleterious in S phase. Overall, the telomere delocalization phenotype of *ctf18* is reminiscent of that described for *yku70*, which has been reported to affect the positioning of some telomeres primarily during G1 (Hediger et al, 2002).

We performed time-lapse analysis to examine whether delocalized telomeres in *ctf18* nuclei can still visit the nuclear periphery. Tracings of movies showing the typical behavior of telomere XIVL in wild-type and *ctf18* cells are shown in Figure 3C (Movies in Supplementary information). In wild-type G1 phase cells (Sup_3.mpg), telomere XIVL remained confined within 0.2 μm of the periphery for most of the analysis. Although the telomere did occasionally leave the nuclear envelope, it returned to the periphery after a short time and usually remained there. In S phase, telomere movement became still more confined, suggesting even more stable localization (Sup_4.mpg). These data are consistent with previous observations in wild-type cells (Heun et al, 2001b). In *ctf18* cells in contrast, telomere XIVL was not confined to nuclear periphery but spent more time in the interior, particularly during G1 phase (Sup_5.mpg). The telomere was not excluded from the edge of the nucleus and did pay occasional visits to the periphery, but failed to become stably localized during those visits. Once *ctf18* cells entered S phase, brief periods of telomere positioning at the periphery were observed, although these were still not of the duration or

stability seen in wild-type S phase cells (Sup_6.mpg).

We measured the duration of localization events (Figure 3D). In unbudded and small-budded *ctf18* mutant cells, periods of internal localization and brief visits to the periphery were increased at the expense of stable peripheral localization periods, to the extent that long-term (greater than 1 minute) localization periods were almost never observed. We conclude that Ctf18-RLC is important for telomere positioning in both G1 and S phase, and that its primary role is to permit the establishment of stable localization at the nuclear periphery.

Telomeres replicate at the normal time in a ctf18 *mutant strain*

S. cerevisiae telomeres are normally late-replicating and are localized at the nuclear periphery. Our discovery of a new effector of telomere localization enabled us to investigate whether peripheral localization of telomeres during G1 is a prerequisite for their late replication. We examined the replication program of a *ctf18* strain using the dense isotope transfer technique (Donaldson et al, 1998). Figure 4A shows the replication programs of wild-type, *ctf18* and *yku70* mutant cells analyzed by using this method. Markers for early and late replication in S phase are provided by the early replication origin *ARS305* and a late-replicating sequence on chromosome XIV that lies far from either telomere (chr XIV-int). We examined the replication time of telomere VIIIL, whose perinuclear localization depends on Ctf18 as shown in Figure 2B. We found that telomere VIIIL replicated late in the *ctf18* mutant as in wild-type cells (Figure 4A, left and centre panels). This result contrasts with the situation in the *yku70* mutant in which telomere VIIIL replicated much earlier in S phase (Figure 4A, right panel). To measure an 'average' telomere replication time, we examined the replication time of the *Y'* sequences. *Y'* is one of the repeated sequence elements found at more than half of yeast telomeres, so that examining *Y'* replication time gives a good view of overall telomere

replication time. *Y'* sequences replicated late in the *ctf18* mutant as in wild-type cells. In the *yku70* mutant, *Y'* sequences replicated much earlier in S phase as shown previously (Cosgrove et al, 2002). A replication time can be assigned for a sequence as the time at which half the final level of replication has occurred, and the interval between the replication of the early and late marker sequences can be taken as a measure of S phase length. In the *ctf18* strain this interval was 16.4 min for the experiment shown in Figure 4A, compared with 23.8 min in the wild-type and 19.7 min in the *yku70* mutant strain. The S phase program may therefore be slightly compressed in the *ctf18* strain. 'Replication index' (RI) values can be calculated to compare the replication programs in different strains and adjust for differences in the speed at which cultures release from synchrony. RI values express the time of replication of each sequence as a proportion of elapsed S phase. Figure 4B shows the replication programs of wild-type, *ctf18*, and *yku70* strains plotted according to replication index. In this format it is clear that there is no significant change in the relative replication time of Y' sequences in the *ctf18* strain when compared to wild-type. Analysis of two additional loci (sequences close to the left ends of chromosomes III and VI) also confirmed that the RI values in the *ctf18* S phase were very similar to wild-type, any slight differences observed lying within experimental error.

From these experiments we conclude that the telomeric DNA of a *ctf18* mutant replicates at its normal, late time in S phase despite the aberrant subnuclear localization of the chromosome ends during G1 phase. Our observation of telomere delocalization combined with normal replication timing in the *ctf18* strain shows that peripheral positioning of telomeres during G1 is not essential for their late replication.

Ku complex remains bound to a telomere in a ctf18 *strain*

The telomere positioning phenotype of *ctf18* resembles that reported for *yku70* and *yku80*

mutants (Hediger et al, 2002). Normal telomeric replication timing in the *ctf18* mutant suggested that Ku binding to telomeres is intact, but we wished to test directly whether Ku is loaded onto telomeres in the *ctf18* strain. We examined binding of Myc-tagged Yku80 protein to two loci in the vicinity of telomere VIR. Yku80-Myc was bound at the telomeric sequence, but not to the locus 5 kb away from telomere (Figure 5A), consistent with previous studies (Martin et al, 1999; Roy et al, 2004). We observed no significant change in this telomere-specific binding in the *ctf18* mutant, showing that Ctf18 is not required for Ku binding to chromosome VIR. Yku70 was required for Yku80 to bind the telomere, as expected since Ku binds DNA as a heterodimer. Consistent with the observation that Ku still binds telomeres in *ctf18*, the *ctf18* mutant has only a slight defect in telomere length control (data not shown; Askree et al, 2004; Smolikov et al, 2004), while *yku70* mutant displays a severe telomere length defect (Boulton and Jackson, 1996; Porter et al, 1996).

We tested whether Ctf18 itself is localized at telomeres. Immunofluorescence and *in vivo* labeling experiments gave no suggestion that Ctf18 is specifically located at telomere clusters (data not shown). The higher sensitivity technique of chromatin immunoprecipitation also provided no evidence for Ctf18 binding specifically to telomere VIR (Figure 5B). It therefore seems unlikely that Ctf18 is a structural component of a telomere peripheral localization pathway, and we believe that it is more likely to play a regulatory role.

CTF18 *is required for both Ku and Sir4-mediated telomere positioning pathways during G1*

Two molecular pathways have been described that mediate localization of telomeres. Ku complex is believed to form a link between telomeres and the nuclear envelope by binding to an unidentified envelope-bound component. A second pathway involves interaction of the telomere-bound Sir4 protein with the nuclear envelope-bound protein Esc1. To clarify whether Ctf18-RLC affects telomere positioning through the Ku pathway, through the

Sir4-Esc1 pathway, or through a previously unidentified pathway, we studied the localization of telomere XIVL in a set of double mutants. This telomere was chosen for analysis because it requires both Ku- and Sir4-dependent pathways for full positioning (Figure 6A); many other telomeres show more complete disruption of positioning on deletion of either of the known pathways (Hediger et al, 2002; Taddei et al, 2004a), which could obscure additional effects of further mutations.

Telomere XIVL positioning was random during G1 phase in the *sir4 yku70* mutant (Figure 6A), showing that during G1 the Ku and Sir positioning mechanisms are the only pathways involved in localizing this telomere. Either the *sir4* or *yku70* mutations alone resulted in significant peripheral positioning (Figure 6A), demonstrating that each pathway can mediate some positioning independent of the other—that is, in the absence of Sir4, the Ku pathway can position telomere XIVL to some extent and *vice versa*. However, introducing the *ctf18* mutation in the *sir4* background (Figure 6A, *ctf18 sir4*) resulted in completely random telomere positioning, showing that without Ctf18 the Ku pathway can no longer mediate any telomere positioning. Introducing the *ctf18* mutation into the *yku70* background also resulted in random telomere positioning, showing that Ctf18 is also required for the residual telomere positioning by the Sir pathway in the *yku70* mutant. These results suggest that, at least for telomere XIVL, both the Ku and Sir positioning pathways are largely dependent on Ctf18. This interpretation is consistent with the observation that disruption of *CTF18* leads to a more severe positioning defect than either the *sir4* and *yku70* mutations alone (Figure 6A).

We also examined the effects of the various mutations on telomere positioning during S phase. In this case, the *ctf18* mutant retained a significantly higher level of telomere XIVL positioning than the *sir4 yku70* double mutant (Figure 6A). One interpretation of this result might be that during S phase the Ku and Sir positioning pathways are less dependent on Ctf18 than they are in G1. However, during S phase, significant telomere positioning

remained in the *sir4 yku70* double mutant (Figure 6A) suggesting that an additional telomere positioning pathway plays a role at this cell cycle stage. It is intriguing to speculate that this additional pathway could be related to S phase events such as telomere replication or telomerase extension. Because the components of this additional pathway are unidentified, it is not possible to assess from our results whether Ctf18 is required for this novel positioning mechanism, or whether instead the dependence of the Ku and Sir4 pathways on Ctf18 is altered during S phase. Further clarification will require the identification of components of the S phase-specific Ku/Sir-independent positioning pathway.

CTF18 *is not required for Ku-mediated and Sir4-mediated linkage of an internal locus to the nuclear periphery*

The double mutant analysis showed that, at least during G1, the Ku and Sir-mediated telomere positioning pathways are largely dependent on Ctf18. Taddei et al (2004a) developed a system that allows artificial tethering of an internally-located locus to the nuclear periphery. We wished to examine whether localization of an internal site requires Ctf18, or whether instead it can occur in the absence of Ctf18. We used a strain in which the early replication origin locus *ARS607* is flanked by *lexA* operators (to permit tethering by LexA-Sir4^{PAD} or by LexA-yku80-9) and by a series of *lac* operator sequences (to enable visualization using LacI-GFP) (Figure 6B). The *ARS607* locus is randomly located in a strain bearing this lac_{op}-$lexA_{op}$-*ARS607* construct if no LexA fusion protein is expressed. As described previously, expression of LexA-yku80-9 leads to significant localization of *ARS607* to the nuclear envelope (Figure 6C). The LexA-yku80-9 construct was still able to localize *ARS607* when *CTF18* was deleted. Similarly, the localization mediated by LexA-Sir4^{PAD} was not affected in the *ctf18* mutant (Figure 6D). χ^2 analysis confirmed that the *ctf18* mutation has no significant effect (Table II). Function of the Ctf18-RLC is therefore not required for Yku80

and Sir4 to bring about the peripheral localization of a chromosomal domain. We conclude that tethering of an ectopic locus to the nuclear periphery by either Yku80 or $Sir4^{PAD}$ bypasses the need for Ctf18.

Discussion

We have found that the Ctf18-Replication Factor C-like Complex is critical for correct positioning of *S. cerevisiae* telomeres close to the nuclear periphery, particularly during G1 phase. Our findings represent the discovery of a new molecular effector of chromosome localization, and the identification of a new role for the Ctf18-RLC in intranuclear organization. In mutants in any of the three of the subunits unique to the Ctf18-RLC (Ctf18, Dcc1, and Ctf8) we observed two phenotypes that indicate disrupted telomere organization—the dislodgement of individual chromosome ends from the nuclear periphery and the dispersal of Rap1 from its normal localization pattern in foci within the nucleus. The Ctf18-RLC is unique amongst the three known alternative RFC complexes in having this function in chromosome positioning.

The telomere localization defect in a *ctf18* mutant provided the opportunity to test one model for replication timing control. Several studies had suggested a close relationship between late replication and peripheral positioning of the DNA during G1 phase (Dimitrova and Gilbert, 1999; Heun et al, 2001a). In particular, deletion of the Yku70 subunit of the Ku heterodimer dislodges telomeres from the nuclear periphery, and simultaneously causes aberrantly early activation of telomere-proximal replication origins during S phase (Cosgrove et al, 2002; Laroche et al, 1998). Mutation of the Sir proteins causes a less dramatic but still noticeable disruption of telomere localization, and a slight but significant advancement in telomere replication timing (Stevenson and Gottschling, 1999). The *ctf18* mutation clearly abolishes telomere localization to the nuclear periphery during G1, but we found that the

telomeres of *ctf18* cells replicate at their normal late time in S phase, quite unlike the aberrant early telomere replication observed in a *yku70* mutant. The *ctf18* mutant phenotype therefore demonstrates that peripheral localization during G1 is not a prerequisite for the late replication of telomeres, and shows that the mechanisms of replication timing control must be distinct from those controlling G1 telomere intranuclear positioning.

By what mechanism does the Ctf18-RLC affect telomere positioning? This question is difficult to address while the precise molecular role of the Ctf18-RLC remains unclear. *ctf18* mutants are slightly compromised in mating-type and telomeric silencing (Suter et al, 2004), but the most prominent previously reported phenotype of *ctf18* is premature separation of sister chromatids (Hanna et al, 2001; Mayer et al, 2001; Naiki et al, 2001). We found that cohesin mutants show only a slight defect in telomere XIVL positioning under conditions where the sister chromatid separation defect is clear (data not shown). Moreover, not all mutants that affect sister chromatid cohesion compromise telomere positioning. For example, *CHL1* is required for cohesion (Petronczki et al, 2004; Skibbens, 2004), but the *chl1* mutation did not compromise telomere peripheral positioning as assessed by Rap1 localization and analysis of a tagged telomere (data not shown). Taking these results together, we have found no convincing evidence that the effect of *ctf18* on telomere positioning is a consequence of defective sister chromatid cohesion.

Two independently acting telomere positioning mechanisms have been characterized in budding yeast—the Ku-dependent and Sir4/Esc1-dependent pathways. Ctf18 is required for the full activity of both pathways (Fig. 6A). Ctf18-RLC is not required to load the Ku complex (Figure. 5A), and chromatin fractionation experiments (not shown) gave no suggestion that the association of Ku with chromatin is altered in a *ctf18* mutant strain. *ctf18* and *dcc1* strains retain significant telomeric silencing (Suter et al, 2004), implying that Sir and Rap1 loading onto telomeres (which is essential for telomeric silencing) is not severely

compromised. Since it does not seem to be required to load Ku or Sir complexes, Ctf18-RLC must presumably play a regulatory role to activate telomere positioning by the Ku and Sir-dependent pathways. Ku or Sir fragments tethered to an internal locus are capable of re-positioning that chromosome domain in a *ctf18* mutant, showing that isolated fragments can bypass the need for Ctf18-RLC to activate peripheral positioning (Fig. 6). These results are consistent with models in which Ctf18-RLC 'unmasks' the inherent positioning capability of telomeric chromatin. The requirement for Ctf18 for localization of telomeres therefore probably reflects a particular characteristic of telomeric chromatin, such as the need for a regulatory modification to telomeric chromatin to establish its competence for linkage to the periphery. For example, a post-translational modification of another telomeric protein (such as Rap1) might be required to allow linkage of telomeric heterochromatin to the nuclear periphery by Ku and Sir proteins.

The role of Ctf18 in regulating telomere positioning is doubly mysterious since the Ctf18-RLC is proposed to act at replication forks during S phase (see below) whereas the *ctf18* mutation is most deleterious to telomere positioning during G1 phase. It would be informative to test whether the presence of Ctf18-RLC during DNA replication is required for telomere positioning in the subsequent G1 and S phase.

What is the relationship between the regulatory role of Ctf18-RLC in telomere positioning and the molecular function of RFC-like complexes? Replication Factor C itself loads the ring-shaped sliding clamp PCNA onto replication forks, while Rad24-RLC loads the ring-shaped '9-1-1 complex'. By analogy Ctf18-RLC is believed to load or unload a ring complex. Yeast Ctf18-RLC can unload PCNA from DNA very efficiently *in vitro* (Bylund and Burgers, 2005), and PCNA unloading after DNA synthesis is the clearest suggestion for the biochemical function of Ctf18-RLC (Bylund and Burgers, 2005). However, it is not obvious why compromised PCNA unloading should lead to either telomere depositioning or

defective sister chromatid cohesion. It is noteworthy that the Ctf8 and Dcc1 subunits of Ctf18-RLC are required for telomere positioning (Figure 2) and establishment of cohesion (Hanna et al, 2001; Mayer et al, 2001) but dispensable for *in vitro* PCNA unloading. Perhaps Ctf18-RLC has two activities, and the apparently unrelated *in vitro* and *in vivo* observations of its properties reflect different aspects of its function. We suggest that PCNA unloading by Ctf18-RLC might be coupled *in vivo* to another chromatin modification that is required to activate the Ku and Sir telomere positioning pathways in the subsequent G1 phase. Unlike the PCNA-unloading step, the second, coupled step would be expected to require Ctf8 and Dcc1 since these subunits are required for telomere positioning. One possibility is that the second activity of Ctf18-RLC involves loading of another ring-shaped complex.

Ctf18-RLC could conceivably play a related role at other chromosomal loci—for example, to establish cohesin loading sites as competent for sister chromatid attachment. If so, Ctf18-RLC might be envisaged as having a general involvement in activating particular properties of specialized chromatin sites following DNA replication. It will be of interest to investigate whether the complex is involved in regulating chromosome organization within mammalian nuclei.

Materials and Methods

Yeast strains

Gene deletion collections were purchased from EUROSCARF. Other strains are described in Supplementary information.

Plasmids

Plasmid pAT4-yku80-9 (encoding Yku80-9 fused to LexA) and pAT4-Sir4^{PAD} (encoding

Sir4^{PAD} fused to LexA) were as described (Taddei et al, 2004a). Additional plasmids are described in Supplementary information.

Microscopic techniques

Cell cycle classification was as follows: unbudded cells = G1 phase; bud size less than 2 μm = S phase; bud larger than 2μm with round nucleus not at the bud neck = G2; bud larger than 2μm with elongated nucleus at the bud neck = M phase. Microscopic techniques are described in Supplementary information.

Chromatin immunoprecipitation

Chromatin immunoprecipitation of Myc-tagged Yku80 and Ctf18 proteins was performed as described (Strahl-Bolsinger et al, 1997; Tanaka et al, 1997), using monoclonal anti-Myc antibody (9E11) (Abcam). Units of DNA in each PCR reaction were calculated relative to amplification of a dilution series of whole-genomic standard DNA by the same primer pair. Details of primer pairs used are described in Supplementary information.

Analysis of replication timing program

Dense isotope transfer experiments were carried out as described previously (Donaldson et al, 1998) using α-factor synchronization and release at 30ºC in light medium. Probes are described in Supplementary information.

Acknowledgments

Thanks to Luis Aragon, Aki Hayashi-Hagihara, Yasushi Hiraoka, Susan Gasser and Virginia Zakian for materials, and to Tomoyuki Tanaka and Kozo Tanaka for technical advice. Berndt Müller and Conrad Nieduszynski provided comments on the manuscript.

Supplementary information is available at *The EMBO Journal* Online.

References

Andrulis ED, Neiman OM, Zappulla DC, Sternglanz R (1998) Perinuclear localization of chromatin facilitates transcriptional silencing. *Nature* **394**: 592-595

Askree SH, Yehuda T, Smolikov S, Gurevich R, Hawk J, Coker C, Krauskopf O, Kupiec M, McEachern MJ (2004) A genome-wide screen for *Saccharomyces cerevisiae* deletion mutants that affect telomere length. *Proc Natl Acad Sci USA* **101**: 8658-8663

Bermudez VP, Maniwa Y, Tappin I, Ozato K, Yokomori K, Hurwitz J (2003) The alternative Ctf18-Dcc1-Ctf8-replication factor C complex required for sister chromatid cohesion loads proliferating cell nuclear antigen onto DNA. *Proc Natl Acad Sci USA* **100**: 10237-10242

Boulton SJ, Jackson SP (1996) Identification of a *Saccharomyces cerevisiae* Ku80 homologue: roles in DNA double strand break rejoining and in telomeric maintenance. *Nucleic Acids Res* **24**: 4639-4648

Bowman GD, O'Donnell M, Kuriyan J (2004) Structural analysis of a eukaryotic sliding DNA clamp-clamp loader complex. *Nature* **429**: 724-730

Bylund GO, Burgers PM (2005) Replication protein A-directed unloading of PCNA by the Ctf18 cohesion establishment complex. *Mol Cell Biol* **25**: 5445-5455

Bystricky K, Laroche T, van Houwe G, Blaszczyk M, Gasser SM. (2005) Chromosome looping in yeast: telomere pairing and coordinated movement reflect anchoring efficiency and territorial organization. *J Cell Biol* **168**: 375-387

Cosgrove, AJ, Nieduszynski CA, Donaldson AD (2002) Ku complex controls the replication time of DNA in telomere regions. *Genes Dev* **16**: 2485-2490

Dimitrova DS, Gilbert DM (1999) The spatial position and replication timing of chromosomal domains are both established in early G1 phase. *Mol Cell* **4**: 983-993

Donaldson, AD, Raghuraman MK, Friedman KL, Cross FR, Brewer BJ, Fangman WL (1998) *CLB5*-dependent activation of late replication origins in *S. cerevisiae*. *Mol Cell* **2**: 173-182

Ferguson BM, Fangman WL (1992) A position effect on the time of replication origin activation in yeast. *Cell* **68**: 333-339

Gartenberg MR, Neumann FR, Laroche T, Blaszczyk M, Gasser SM (2004) Sir-mediated repression can occur independently of chromosomal and subnuclear contexts. *Cell* **119**: 955-967

Gilbert DM. (2002) Replication timing and transcriptional control: beyond cause and effect. *Curr Opin Cell Biol* **14**: 377-383

Gilbert N, Boyle S, Fiegler H, Woodfine K, Carter NP, Bickmore WA (2004) Chromatin architecture of the human genome: gene-rich domains are enriched in open chromatin fibers. *Cell* **118**: 555-566

Gotta M, Laroche T, Formenton, A, Maillet L, Scherthan H, Gasser SM (1996) The clustering of telomeres and colocalization with Rap1, Sir3, and Sir4 proteins in wild-type *Saccharomyces cerevisiae*. *J Cell Biol* **134**: 1349-1363

Gottschling DE, Aparicio OM, Billington BL, Zakian VA (1990) Position effect at S. cerevisiae telomeres: reversible repression of Pol II transcription. *Cell* **63**: 751-762

Gravel S, Larrivee M, Labrecque P, Wellinger RJ (1998) Yeast Ku as a regulator of chromosomal DNA end structure. *Science* **280**: 741-744

Hanna JS, Kroll ES, Lundblad V, Spencer FA (2001) *Saccharomyces cerevisiae CTF18* and *CTF4* are required for sister chromatid cohesion. *Mol Cell Biol* **21**: 3144-3158

Hayashi, A, Ogawa H, Kohno K, Gasser SM, Hiraoka Y (1998) Meiotic behaviours of

chromosomes and microtubules in budding yeast: relocalization of centromeres and telomeres during meiotic prophase. *Genes Cells* **3**: 587-601

Hediger F, Neumann FR, Van Houwe G, Dubrana K, Gasser SM (2002) Live imaging of telomeres: yKu and Sir proteins define redundant telomere-anchoring pathways in yeast. *Curr Biol* **12**: 2076-2089

Heun P, Laroche T, Raghuraman MK, Gasser SM (2001a) The positioning and dynamics of origins of replication in the budding yeast nucleus. *J Cell Biol* **152**: 385-400

Heun P, Laroche T, Shimada K, Furrer P, Gasser SM (2001b) Chromosome dynamics in the yeast interphase nucleus. *Science* **294**: 2181-2186

Kenna MA, Skibbens RV. (2003) Mechanical link between cohesion establishment and DNA replication: Ctf7p/Eco1p, a cohesion establishment factor, associates with three different replication factor C complexes. *Mol Cell Biol* **23**: 2999-3007

Kim J, MacNeill SA (2003) Genome stability: a new member of the RFC family. *Curr Biol* **13**: R873-875

Laroche T, Martin SG, Gotta M, Gorham HC, Pryde FE, Louis EJ, Gasser SM (1998) Mutation of yeast Ku genes disrupts the subnuclear organization of telomeres. *Curr Biol* **8**: 653-656

Martin SG, Laroche T, Suka N, Grunstein M, Gasser SM (1999) Relocalization of telomeric Ku and SIR proteins in response to DNA strand breaks in yeast. *Cell* **97**: 621-633

Mayer ML, Gygi SP, Aebersold R, Hieter P (2001) Identification of RFC(Ctf18p, Ctf8p, Dcc1p): an alternative RFC complex required for sister chromatid cohesion in *S. cerevisiae*. *Mol Cell* **7**: 959-970

Merkle CJ, Karnitz LM, Henry-Sanchez JT, Chen J (2003) Cloning and characterization of hCTF18, hCTF8, and hDCC1. Human homologs of a *Saccharomyces cerevisiae* complex involved in sister chromatid cohesion establishment. *J Biol Chem* **278**:

30051-30056

Naiki T, Kondo T, Nakada D, Matsumoto K, Sugimoto K (2001) Chl12 (Ctf18) forms a novel replication factor C-related complex and functions redundantly with Rad24 in the DNA replication checkpoint pathway. *Mol Cell Biol* **21**: 5838-5845

Ohta S, Shiomi Y, Sugimoto K, Obuse C, Tsurimoto T (2002) A proteomics approach to identify proliferating cell nuclear antigen (PCNA)-binding proteins in human cell lysates. Identification of the human CHL12/RFCs2-5 complex as a novel PCNA-binding protein. *J Biol Chem* **277**: 40362-40367

Palladino F, Laroche T, Gilson E, Axelrod, A, Pillus L, Gasser SM (1993) SIR3 and SIR4 proteins are required for the positioning and integrity of yeast telomeres. *Cell* **75**: 543-555

Petronczki M, Chwalla B, Siomos MF, Yokobayashi S, Helmhart W, Deutschbauer, AM, Davis RW, Watanabe Y, Nasmyth K (2004) Sister-chromatid cohesion mediated by the alternative RF-$C^{Ctf18/Dcc1/Ctf8}$, the helicase Chl1 and the polymerase-alpha-associated protein Ctf4 is essential for chromatid disjunction during meiosis II. *J Cell Sci* **117**: 3547-3559

Porter SE, Greenwell PW, Ritchie KB, Petes TD (1996) The DNA-binding protein Hdf1p (a putative Ku homologue) is required for maintaining normal telomere length in *Saccharomyces cerevisiae*. *Nucleic Acids Res* **24**: 582-585

Raghuraman MK, Brewer BJ, Fangman WL (1997) Cell cycle-dependent establishment of a late replication program. *Science* **276**: 806-809

Raghuraman MK, Winzeler EA, Collingwood D, Hunt S, Wodicka L, Conway, A, Lockhart DJ, Davis RW, Brewer BJ, Fangman WL (2001) Replication dynamics of the yeast genome. *Science* **294**: 115-121

Roy R, Meier B, McAinsh, AD, Feldmann HM, Jackson SP (2004) Separation-of-function

mutants of yeast Ku80 reveal a Yku80p-Sir4p interaction involved in telomeric silencing. *J Biol Chem* **279**: 86-94

Skibbens RV (2004) Chl1p, a DNA helicase-like protein in budding yeast, functions in sister-chromatid cohesion. *Genetics* **166**: 33-42

Smolikov S, Mazor Y, Krauskopf, A (2004) ELG1, a regulator of genome stability, has a role in telomere length regulation and in silencing. *Proc Natl Acad Sci USA* **101**: 1656-1661

Stellwagen AE, Haimberger ZW, Veatch JR, Gottschling DE (2003) Ku interacts with telomerase RNA to promote telomere addition at native and broken chromosome ends. *Genes Dev* **17**: 2384-2395

Stevenson JB, Gottschling DE. (1999) Telomeric chromatin modulates replication timing near chromosome ends. *Genes Dev* **13**: 146-151

Strahl-Bolsinger S, Hecht, A, Luo K, Grunstein M (1997) SIR2 and SIR4 interactions differ in core and extended telomeric heterochromatin in yeast. *Genes Dev* **11**: 83-93

Straight, AF, Belmont, AS, Robinett CC, Murray, AW. (1996) GFP tagging of budding yeast chromosomes reveals that protein-protein interactions can mediate sister chromatid cohesion. *Curr Biol* **6**: 1599-1608.

Suter B, Tong, A, Chang M, Yu L, Brown GW, Boone C, Rine J (2004) The origin recognition complex links replication, sister chromatid cohesion and transcriptional silencing in *Saccharomyces cerevisiae*. *Genetics* **167**: 579-591

Taddei, A, Hediger F, Neumann FR, Bauer C, Gasser SM (2004a) Separation of silencing from perinuclear anchoring functions in yeast Ku80, Sir4 and Esc1 proteins. *Embo J* **23**: 1301-1312

Taddei, A, Hediger F, Neumann FR, Gasser SM (2004b) The Function of Nuclear Architecture: A Genetic Approach. *Annu Rev Genet* **38**: 305-345

Tanabe H, Habermann FA, Solovei I, Cremer M, Cremer T (2002) Non-random radial arrangements of interphase chromosome territories: evolutionary considerations and functional implications. *Mutat Res* **504**: 37-45

Tanaka T, Knapp D, Nasmyth K (1997) Loading of an Mcm protein onto DNA replication origins is regulated by Cdc6p and CDKs. *Cell* **90**: 649-660

Tham WH, Wyithe JS, Ko Ferrigno P, Silver PA, Zakian VA (2001) Localization of yeast telomeres to the nuclear periphery is separable from transcriptional repression and telomere stability functions. *Mol Cell* **8**: 189-199

Woodfine K, Fiegler H, Beare DM, Collins JE, McCann OT, Young BD, Debernardi S, Mott R, Dunham I, Carter NP (2004) Replication timing of the human genome. *Hum Mol Genet* **13**: 191-202

Figure Legends

Figure 1. *CTF18*, *CTF8*, and *DCC1* are required for formation of Rap1 foci at the nuclear rim. Wild-type, *yku70*, *ctf18*, *ctf8*, *dcc1*, *elg1* and *rad24* strains were transformed with plasmid YCp-GFP-RAP1 and examined by fluorescence microscopy. The 'whole-nucleus' patterns of GFP fluorescence shown in the lower panels were created by capturing images of GFP fluorescence at 250 nm intervals and projecting the Z-stack series of images onto a single plane. Scale bar = 5 μm.

Figure 2. *CTF18*, *CTF8*, and *DCC1* are required for telomere peripheral positioning. (A) Typical images of telomere VIIIL dot in wild-type (GA-1986), *yku70* (SHY120), *ctf18* (SHY117), *ctf8* (SHY118), and *dcc1* (SHY119) strains. Single bright dots in lower panels represent the left telomere of chromosome VIII. The encircling ring of dimmer fluorescence corresponds to the nuclear envelope marked by Nup49-GFP. Scale bar, 5μm. (B) Quantification of telomere position in asynchronous cultures. The position of telomeres VIR, VIIIL, or XIVL was analyzed in wild-type, *ctf18*, *ctf8*, *dcc1* and *yku70* strains. Cells were scored if the telomere dot was located in one of the equatorial Z sections. If the distance between telomeric dot and nuclear rim was less than 230 nm, it was scored as 'nuclear peripheral'. Error bars indicate standard deviations obtained from at least two independent cultures.

Figure 3. Effect of *CTF18* on telomere XIVL positioning in G1 and S phase. (A) Cartoon of zoning analysis. Nuclei with telomeres at the equatorial Z section were divided into 3 concentric zones with equal surface area as shown, and the position of the telomere dot was scored. (B) Analysis of position of telomere XIVL in wild-type (GA-1985) and *ctf18* (SHY114) strains. Histograms show the distribution of telomere dots to the 3 zones,

with Zone 1 the most peripheral. The dotted line in each plot represents random distribution. (C) Telomere movement is less constrained in *ctf18* strain. The movement of telomere XIVL in wild-type and *ctf18* cells was analyzed during G1 and S phase. Red lines show track of telomere XIVL dots over a 6 min period. Green circles represent the nuclear rim. (D) The duration of telomere XIVL peripheral localization events was analyzed in wild-type and *ctf18* strains. The total number of scored time points was 37 for wild-type G1, 42 for wild-type S, 50 for *ctf18* G1, and 35 for *ctf18* S.

Figure 4. Telomeres replicate at the normal time in a *ctf18* strain. Replication timing programs of wild-type, *ctf18*, and *yku70* strains were analyzed using the density transfer technique. (A) Replication kinetics of *ARS305*, chromosome XIV-internal, telomere VIIIL, and subtelomeric *Y'* sequences are shown for each strain. Percentage of cells that have replicated the various loci is plotted against time after release from α-factor. (B) Replication index values of internal (*ARS305*, chr XIV-internal, *ARS1*) and telomere-associated (*Y'*, telomeres VIIIL, VIL, and IIIL) sequences. For wild-type and *ctf18* strains, the standard deviation obtained in two independent experiments is indicated by horizontal error bars. For *yku70*, the density-transfer procedure was carried out only once using this synchronization protocol to illustrate the effect on telomere replication timing described previously (Cosgrove et al, 2002).

Figure 5. Ku binds telomere VIR in a *ctf18* mutant, and Ctf18 does not bind specifically to telomeres. Chromatin immunoprecipitation followed by quantitative PCR was used to examine binding of Yku80-Myc and Ctf18-Myc to loci in the vicinity of chromosome VIR. Histogram keys shows the tagged protein and any further mutation in each strain examined. (A) Telomere binding of Yku80 in a *ctf18* strain. Binding of Yku80 to telomere VIR appeared

similar in wild-type and *ctf18* backgrounds. (B) Ctf18-Myc does not bind specifically to telomere VIR. Amounts of DNA precipitated from Yku80-Myc and non-tagged strains in the same experiments are shown as controls for telomere-specific binding.

Figure 6. The role of Ctf18 in the telomere position machinery. (A) Localization of telomere XIVL was scored in the indicated mutants as in Figure 3B. The proportion of cells having the telomere positioned peripherally (in Zone 1) is plotted for each strain. Error bars indicate standard deviations obtained from at least two independent cultures. Dotted line represents random distribution. (B) The *ARS607* localization construct used to examine Ku and Sir4-mediated tethering. Arrays of lac_{OP} and $lexA_{OP}$ are integrated near *ARS607*. (C) Yku80-mediated tethering of *ARS607* to the nuclear periphery. The position of the *ARS607* locus in WT and *ctf18* strains expressing LexA-yku80-9 fusion protein was scored as in Figure 3. (D) Tethering of *ARS607* mediated by $Sir4^{PAD}$ was examined as in panel (C).

Table I Significance of telomere localization

	P value		
	WT against random[a]	*ctf18* against random[a]	*ctf18* against WT[b]
Telomere XIVL			
G1	2.43×10^{-16}	0.08	5.34×10^{-12}
S	2.22×10^{-21}	1.09×10^{-7}	2.39×10^{-3}
Telomere VIIIL			
G1	2.65×10^{-19}	0.98	6.21×10^{-33}
S	5.92×10^{-13}	8.37×10^{-4}	2.29×10^{-4}

[a]P values were calculated by χ^2 analysis in which actual distribution was compared to a hypothetical random distribution.

[b]P values were calculated by χ^2 analysis in which observed distribution for *ctf18* was compared to that for wild type.

Table II Significance of LexA fusion-dependent tethering

	P value		
	WT against random[a]	*ctf18* against random[a]	*ctf18* against WT[b]
LexA-yku80-9			
G1	5.28×10^{-10}	2.17×10^{-12}	0.18
S	3.15×10^{-6}	6.72×10^{-6}	0.13
LexA-Sir4^{PAD}			
G1	5.88×10^{-5}	2.01×10^{-6}	0.19
S	7.26×10^{-6}	9.07×10^{-7}	0.10

[a]P values were calculated by χ^2 analysis in which actual distribution was compared to a hypothetical random distribution.

[b]P values were calculated by χ^2 analysis in which observed distribution for *ctf18* was compared to that for wild type.

Figure 1

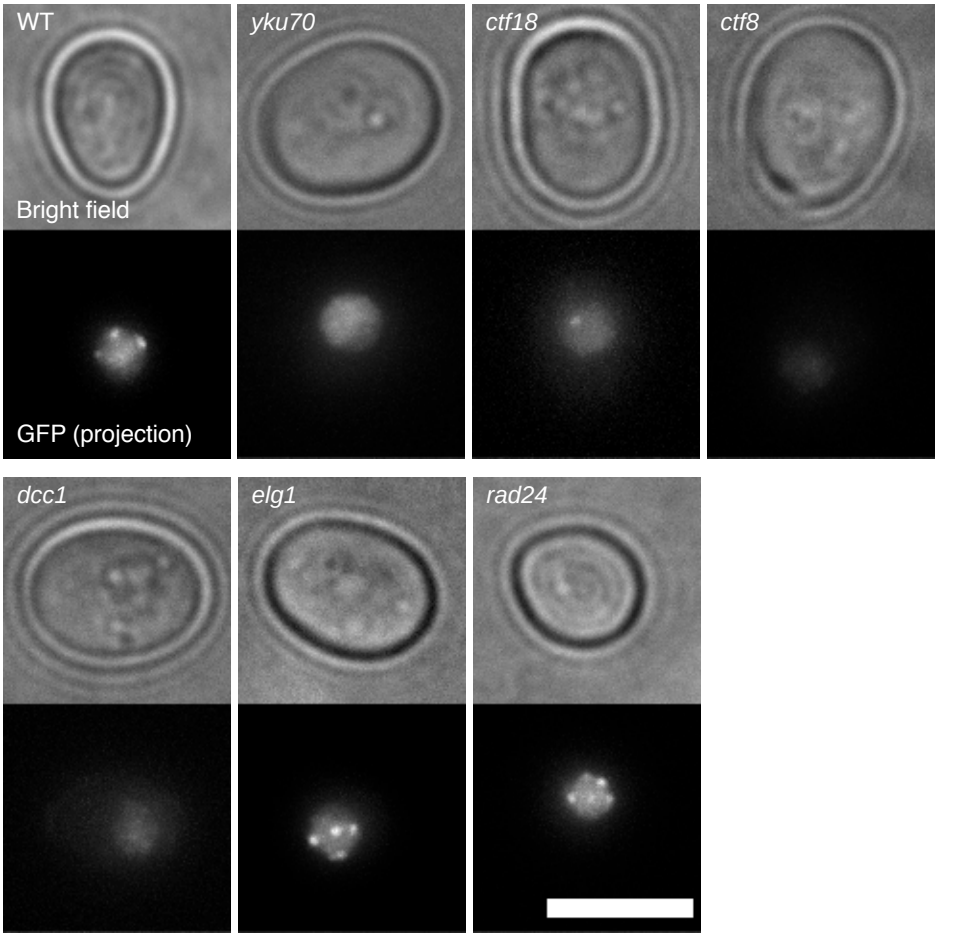
WT
yku70
ctf18
ctf8
Bright field
GFP (projection)
dcc1
elg1
rad24

Figure 2

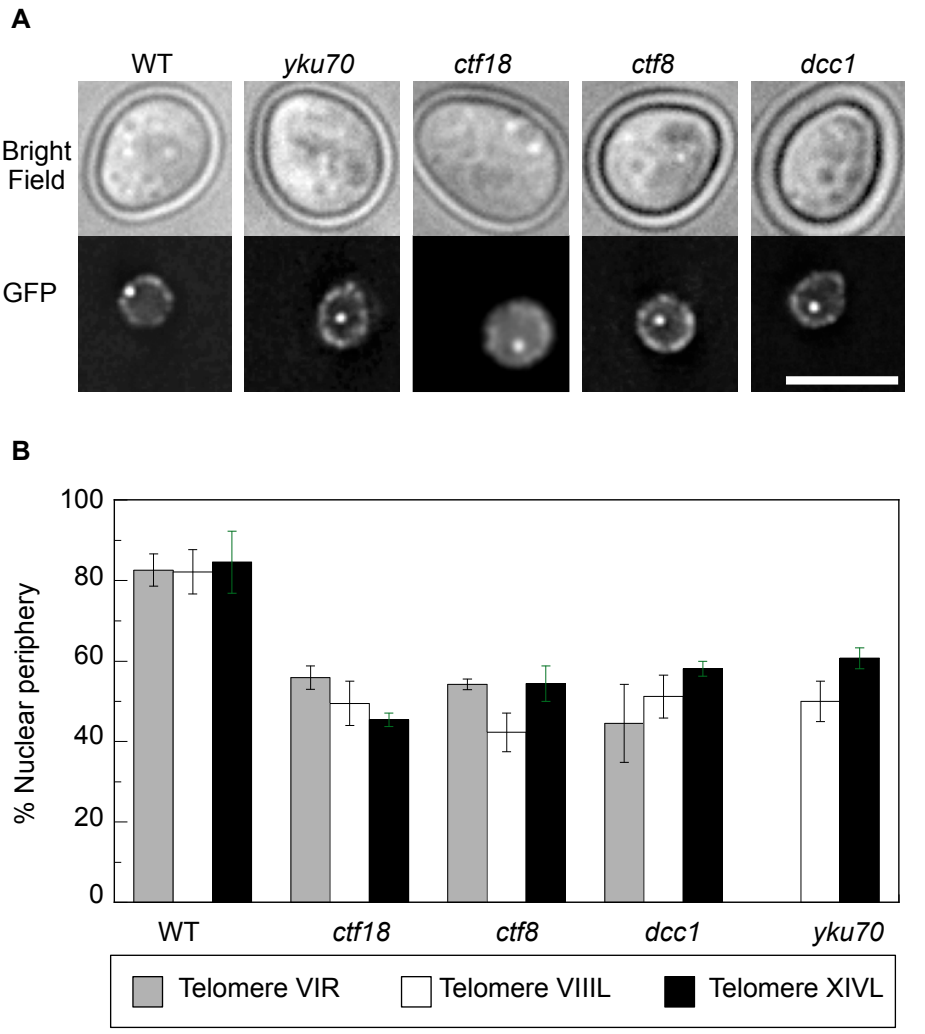
A
WT
yku70
ctf18
ctf8
dcc1
Bright Field
GFP
B
% Nuclear periphery
100
80
60
40
20
0
WT
ctf18
ctf8
dcc1
yku70
Telomere VIR
Telomere VIIIL
Telomere XIVL

Figure 3

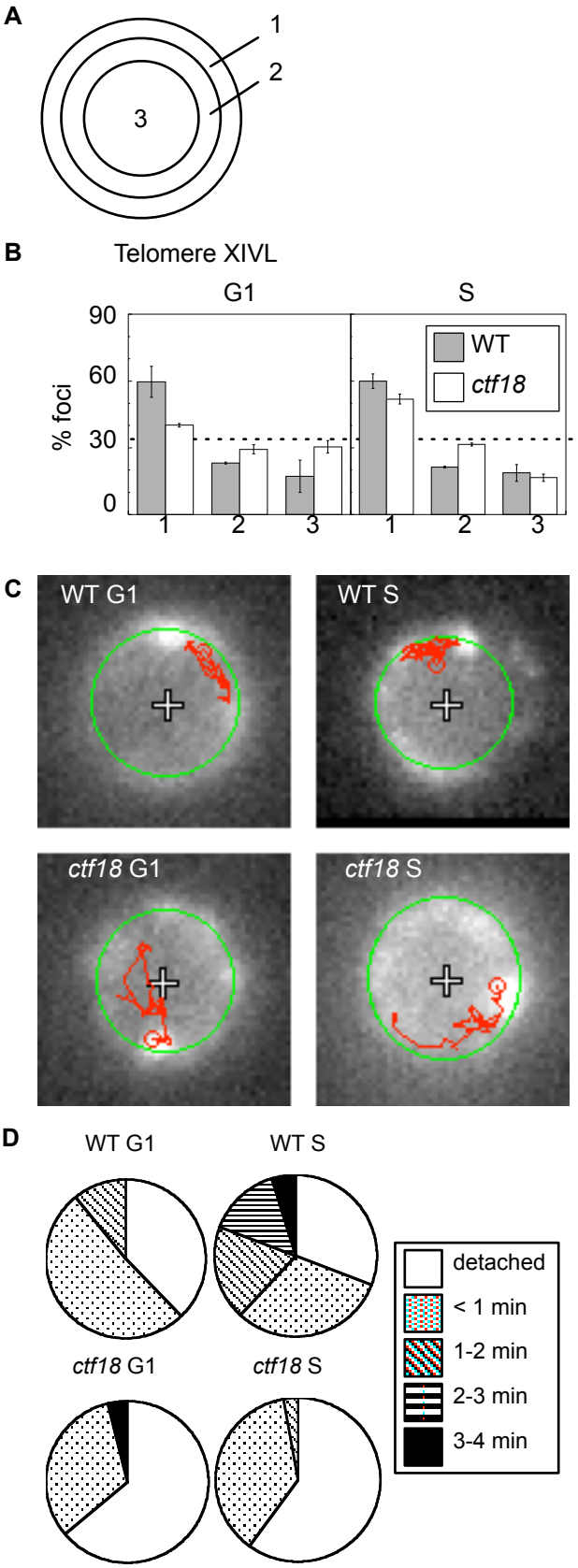
A
1
2
3
B
Telomere XIVL
G1
S
90
60
30
0
% foci
WT
ctf18
1
2
3
1
2
3
C
WT G1
WT S
ctf18 G1
ctf18 S
D
WT G1
WT S
ctf18 G1
ctf18 S
detached
< 1 min
1-2 min
2-3 min
3-4 min

Figure 4

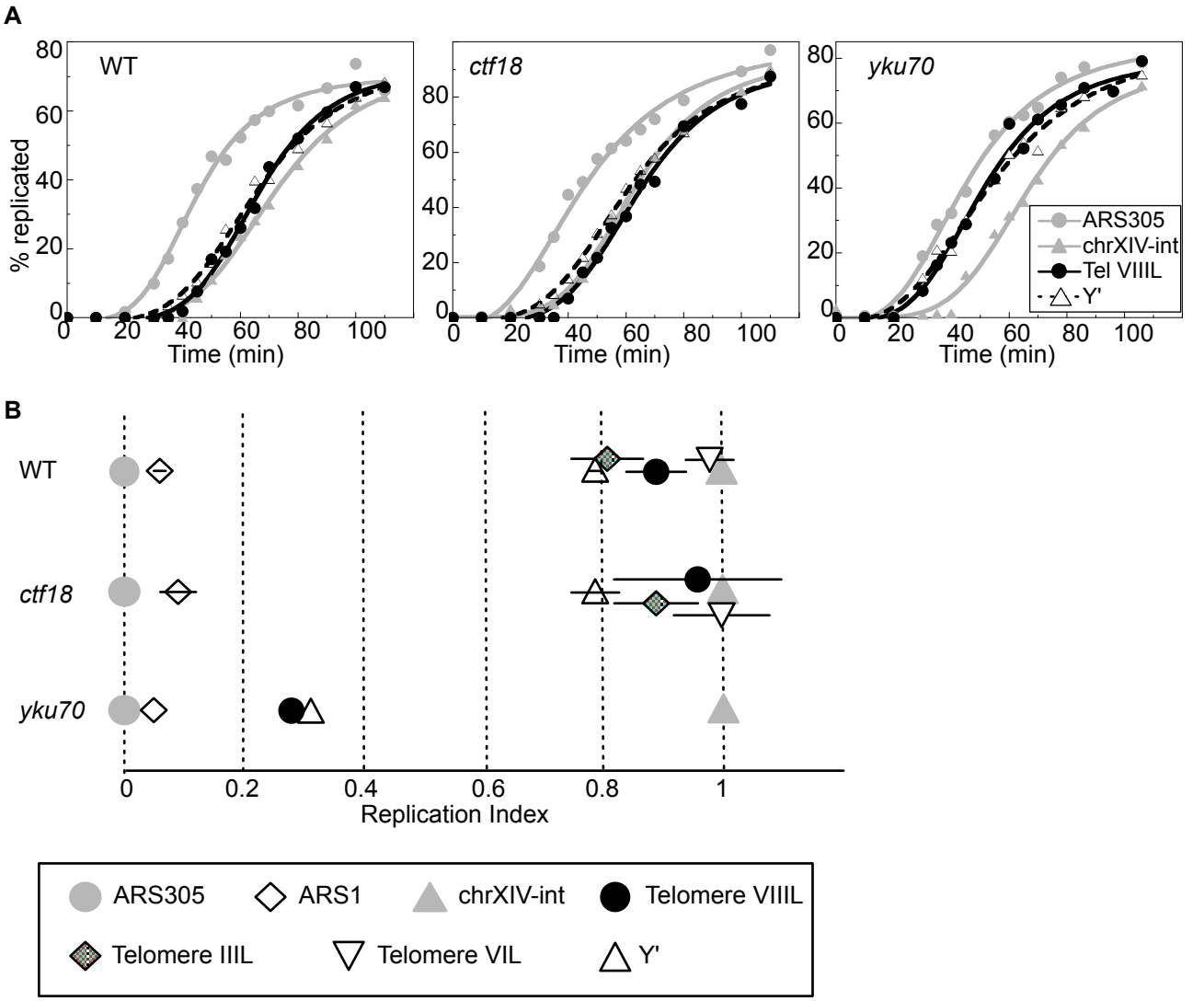
A
WT
ctf18
yku70
% replicated
Time (min)
ARS305
chrXIV-int
Tel VIIIL
Y'
B
WT
ctf18
yku70
Replication Index
ARS305
ARS1
chrXIV-int
Telomere VIIIL
Telomere IIIL
Telomere VIL
Y'

Figure 5

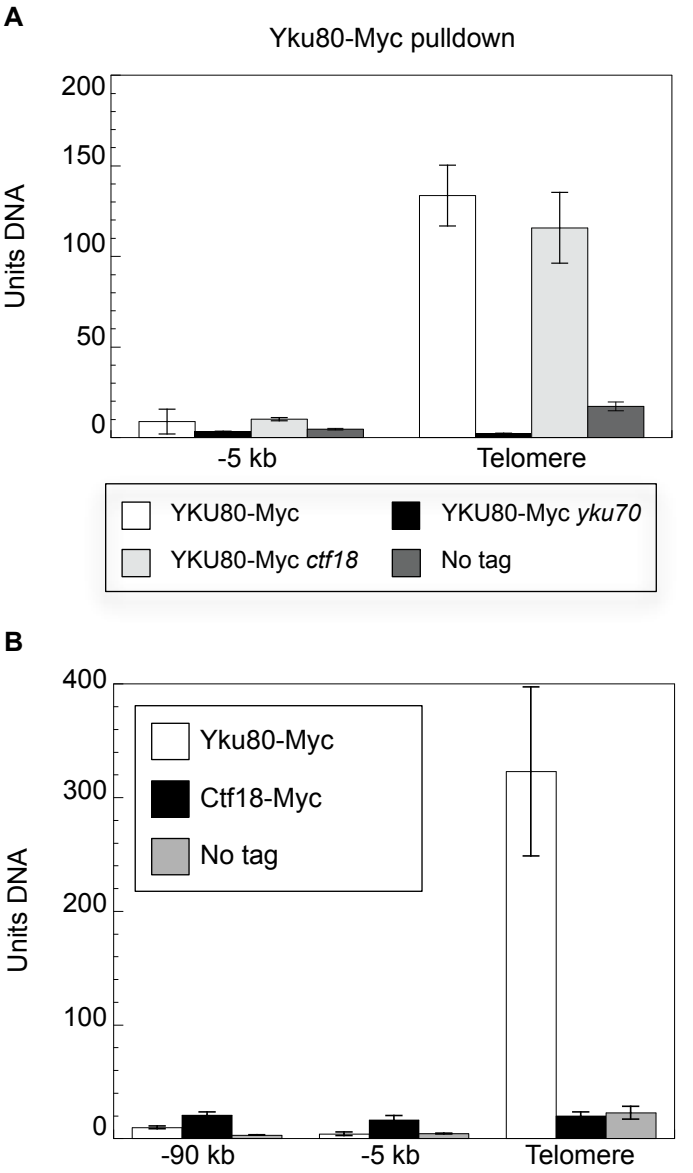
A
Yku80-Myc pulldown
Units DNA
200
150
100
50
0
-5 kb
Telomere
YKU80-Myc
YKU80-Myc yku70
YKU80-Myc ctf18
No tag
B
Units DNA
400
300
200
100
0
Yku80-Myc
Ctf18-Myc
No tag
-90 kb
-5 kb
Telomere

Figure 6

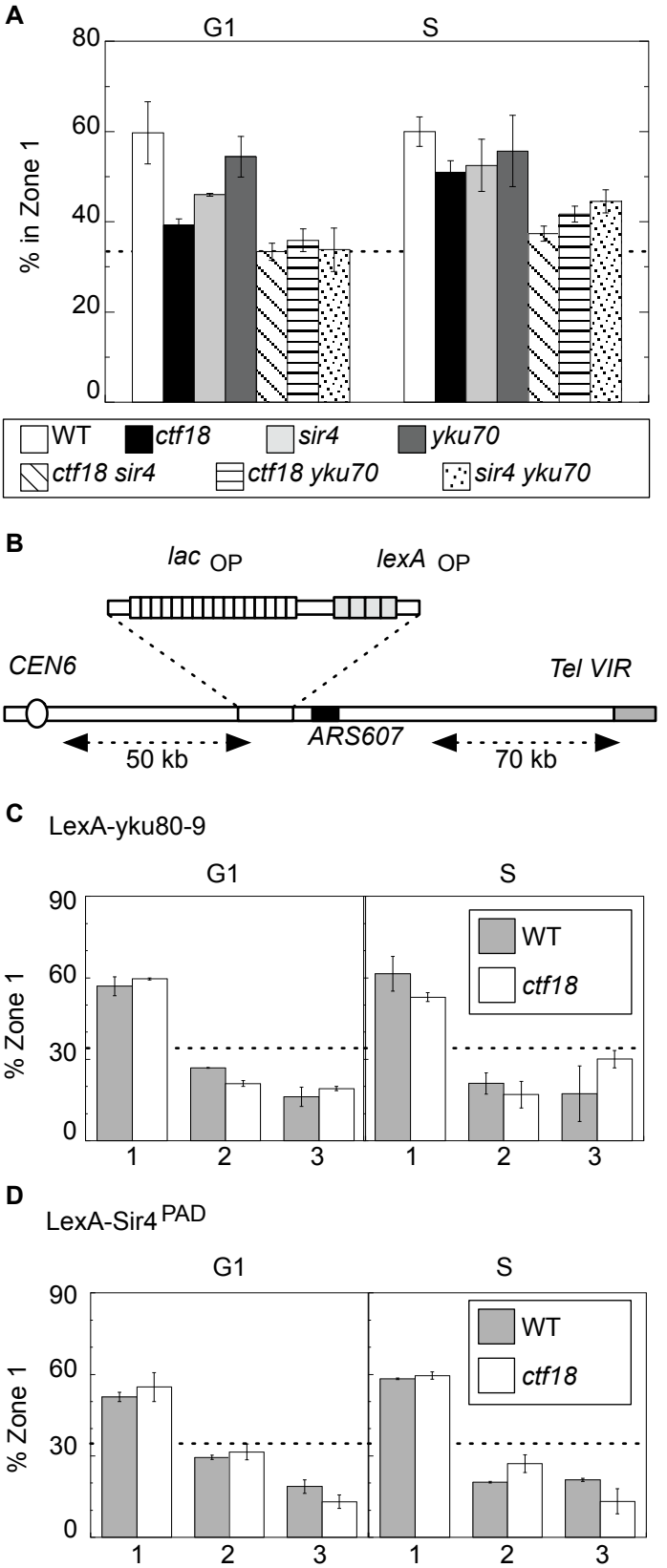
A
G1
S
80
60
40
20
0
% in Zone 1
WT
ctf18
sir4
yku70
ctf18 sir4
ctf18 yku70
sir4 yku70
B
lac OP
lexA OP
CEN6
Tel VIR
ARS607
50 kb
70 kb
C
LexA-yku80-9
G1
S
90
60
30
0
% Zone 1
WT
ctf18
1
2
3
D
LexA-Sir4 PAD
G1
S
90
60
30
0
% Zone 1
WT
ctf18
1
2
3

Supplementary materials and methods.

Plasmids

To construct the YCp-GFP-RAP1 plasmid, the following fragments were ligated: (1) vector backbone from YCplac33 (Gietz and Sugino, 1988) cut with *Xba*I and *Eco*RI (*Eco*RI end was filled), (2) GFP-*RAP1* coding sequence as *Pst*I - *Bss*HII fragment of pAH52 (Hayashi et al, 1998), whose *Bss*HII end was filled by Klenow fragment, and (3) promoter region of *RAP1*, PCR-amplified from W303a genomic DNA then digested at *Xba*I (introduced by PCR) and genomic *Pst*I sites. Plasmid pDM266 (Straight et al, 1999) was obtained from Luis Aragon (MRC Clinical Sciences Centre, UK).

Microscopic techniques

For observations of GFP fluorescence in living yeast cells, cells were grown to log phase, recovered by centrifugation, then resuspended in synthetic complete media. Cells were mounted on an agarose-pad. Z stack images were taken at appropriate intervals using a Deltavison (Applied Precision) with 60x (NA 1.4) or 100x (NA 1.35) objectives. Out-of-focus haze was removed by iterative deconvolution if required.

Quantitative evaluation in Figures 3 and 6 of telomere position was performed essentially as described (Hediger et al, 2002) except that average diameter of the nucleus in each strain at each cell cycle stage (G1, S, and G2) was used to calculate the size of concentric zones. P values were calculated by χ^2 analysis as described in footnotes of Tables I and II.

For time-lapse analysis, a Zeiss Axioplan 2 equipped with ORCA-ER CCD camera (Hamamatsu Photonics) with 100x objective (NA 1.35) was used. GFP and phase contrast

images were captured at 5-sec intervals. ImageJ software (http://rsb.info.nih.gov/ij/) with SpotTracker plug-in (Gartenberg et al, 2004) was used to track telomere movement in Figure 3.

The duration of localization periods of the telomere dot at the nuclear envelope was measured as follows: from a single-section time-lapse series of images where the telomere dot remained approximately in focus, the image at 90 sec was examined and telomere position was scored. If the telomere position was within 170 nm from nuclear envelope (roughly corresponds to Zone 1 in 3-zoning analysis), it was scored as "localized"; otherwise "detached". For the "localized" telomeres, the duration of that localization event was determined by inspecting the telomere position in previous and following time points. Similar measurements were done for images at 180 sec, 270 sec, 360 sec, 450 sec, 540 sec, and 630 sec of all possible time-lapse image series, to obtain the data presented in Figure 3.

Chromatin immunoprecipitation

The amount of DNA immunoprecipated was measured by real-time PCR using DNA Engine Opticon 2 (MJ Research) and DyNamo SYBR Green qPCR kit (Finnzymes). SGD coordinates of the PCR-amplified fragments are 269314 to 269487 (telomere VIR), 264646 to 264839 (5 kb from telomere VIR), and 181173 to 181358 (90 kb from telomere VIR).

Analysis of replication timing program

To analyze replication timing the DNA of cell cultures was first labeled by growth in medium containing dense isotopes of carbon and nitrogen. Cultures were then synchronized in late G1 using α-factor and released in medium containing light isotopes of carbon and nitrogen. Samples were taken throughout S phase and the genomic DNA recovered and digested with

EcoRI before centrifugation on a cesium chloride gradient. The replication kinetics of specific sequences were assessed by monitoring their transition from the heavy-heavy to the heavy-light peak of DNA density. *ARS305* and *ARS1* fragments probed were as described previously (Friedman et al, 1996; McCarroll and Fangman, 1988). Fragments made by PCR amplification of appropriate sequences were used to detect the following *Eco*RI fragments (numbers based on the *Saccharomyces cerevisiae* Genome Database): chromosome XIV-internal (XIV 221459-226536); chromosome VIII-left (VIII 6461-11142), chromosome VI-left (VI 16430-21324); chromosome III-left (III 2052–6585). A 738bp *Hpa*II probe fragment containing the Y' ARS sequence was used to measure replication kinetics of the Y' sequence elements.

Strains

Strains used are listed in the following strain table. To construct *ctf18::kanMX3*, *ctf8::kanMX3*, *dcc1::kanMX3*, and *sir4::kanMX3* strains, *orf::kanMX* constructs were PCR-amplified from relevant EUROSCARF gene deletion strains and transferred to strains GA-1459, GA-1985 and GA-1986. Other gene disruptions and epitope-tagging were performed as described (Longtine et al, 1998); primer sequences available on request.

Table SI. Yeast Strains Used in This study

Name	Relevant genotype	Reference
AW31	*MAT***a** *bar1 ura3-52 trp1-289 leu2-3,112 his6*	Donaldson et al, 1998
BY4741	*MAT***a** *his3Δ leu2Δ0 met15Δ ura3Δ0*	Brachmann et al, 1998
GA-1320	W303-1A *NUP49-GFP his3-15::HIS3p-GFP-lacI-HIS3*	Hediger et al, 2002
GA-1461	GA-1320 *ARS607::lacO-LexAop::TRP1*	Taddei et al, 2004
GA-1459	GA-1320 *TEL VIR::lacO-TRP1*	Hediger et al, 2002
GA-1985	GA-1320 *TEL XIVL::lacO-TRP1*	Hediger et al, 2002
GA-1986	GA-1320 *TEL VIIIL::lacO-TRP1*	Hediger et al, 2002
YK402	W303-1A Δ*bar1*	Araki et al, 2003
SHY146	YPH499 *YKU80-G8-Myc18::TRP1*	Obtained from Zakian lab (Fisher et al, 2004).
DR1	*YKU80-18Myc* Δ*ctf18::HIS3*	This study
DR2	*YKU80-18Myc Δyku70::HIS3*	This study
SHY111	GA-1459 Δ*ctf18::kanMX3*	This study
SHY112	GA-1459 Δ*ctf8::kanMX3*	This study
SHY113	GA-1459 Δ*dcc1::kanMX3*	This study
SHY114	GA-1985 Δ*ctf18::kanMX3*	This study
SHY115	GA-1985 Δ*ctf8::kanMX3*	This study
SHY116	GA-1985 Δ*dcc1::kanMX3*	This study
SHY117	GA-1986 Δ*ctf18::kanMX3*	This study
SHY118	GA-1986 Δ*ctf8::kanMX3*	This study
SHY119	GA-1986 Δ*dcc1::kanMX3*	This study
SHY120	GA-1986 Δ*yku70::kanMX3*	This study
SHY139	GA-1461 Δ*ctf18::kanMX3*	This study
SHY143	BY4741 *NET1-GFP* (pDM266 integrated)	This study
SHY144	SHY143 Δ*ctf18::kanMX3*	This study
SHY145	AW31 Δ*ctf18::kanMX3:: URA3*	This study
SHY152	YK402 *CTF18-13Myc::TRP1*	This study
SHY155	GA-1985 Δ*yku70::URA3*	This study
SHY157	GA-1985 Δ*ctf18::LEU2* Δ*yku70::URA3*	This study
SHY158	GA-1985 Δ*sir4::kanMX3*	This study
SHY159	GA-1985 Δ*ctf18::LEU2* Δ*sir4::kanMX3*	This study
SHY160	GA-1985 Δ*sir4::kanMX3* Δ*yku70::URA3*	This study

Supplementary references

Araki Y, Kawasaki Y, Sasanuma H, Tye BK, Sugino A (2003) Budding yeast mcm10/dna43 mutant requires a novel repair pathway for viability. *Genes Cells* **8**: 465-480

Brachmann CB, Davies A, Cost GJ, Caputo E, Li J, Hieter, P, Boeke JD. (1998) Designer deletion strains derived from *Saccharomyces cerevisiae* S288C: a useful set of strains and plasmids for PCR-mediated gene disruption and other applications. *Yeast* **14**: 115-132

Fisher TS, Taggart AK, Zakian VA. (2004) Cell cycle-dependent regulation of yeast telomerase by Ku. *Nat Struct Mol Biol* **11**: 1198-1205

Friedman KL, Diller JD, Ferguson BM, Nyland SV, Brewer BJ, Fangman WL. (1996) Multiple determinants controlling activation of yeast replication origins late in S phase. *Genes Dev* **10**: 1595-1607

Gietz RD, Sugino A (1988) New yeast-Escherichia coli shuttle vectors constructed with in vitro mutagenized yeast genes lacking six-base pair restriction sites. *Gene* **74**: 527-534

Longtine MS, McKenzie A 3rd, Demarini DJ, Shah NG, Wach A, Brachat A, Philippsen, P, Pringle JR. (1998) Additional modules for versatile and economical PCR-based gene deletion and modification in *Saccharomyces cerevisiae*. *Yeast* **14**: 953-961

McCarroll RM, Fangman WL. (1988) Time of replication of yeast centromeres and telomeres. *Cell* **54**: 505-513

Straight AF, Shou, W, Dowd GJ, Turck CW, Deshaies RJ, Johnson AD, Moazed D (1999) Net1, a Sir2-associated nucleolar protein required for rDNA silencing and nucleolar integrity. *Cell* **97**: 245-256